Research Article

Exploration of weak interactions in penta-substituted cyclohexanol: Crystal structure and DFT study

Sudipta Pathak[a*], **Shibashis Halder**[b], **Malay Dolai**[c] **and Saugata Konar**[d*]

[a]*Department of Chemistry, Haldia Govt. College, Haldia, Purba Medinipur – 721657, India*
[b]*Department of Chemistry, T.N.B. College, Bhagalpur, Bihar – 812007, India*
[c]*Department of Chemistry, Prabhat Kumar College, Purba Medinipur – 721404, India*
[d]*Department of Chemistry, The Bhawanipur Education Society College, Kolkata – 700020, India*

During attempts to produce penta-substituted cyclohexanol involving weak interactions, we have crystallized **A** [where, **A** = (1S,2S,3R,4S,6S)-2,6-bis(4-bromophenyl)-4-hydroxy-4-(pyridin-2-yl)cyclohexane-1,3-diyl)-bis(pyridin-2-ylmethanone)] in DMF-water (1 : 1) solvent mixture with the P-1 space group. Interestingly, in this class of compound, weak interactions have not been explored elaborately in the literature. Herein, we have investigated various types of weak interactions like $\pi \cdots \pi$ interaction, C–H$\cdots \pi$ interaction, Br$\cdots$Br interaction and H-bonding interaction. These types of non-covalent interactions attribute to the supramolecular framework in the crystal packing of the studied molecule. In addition, the composition of the organic molecule **A** is confirmed from Single crystal X-ray structure and then performed the theoretical geometry optimization (DFT study) on it.

Key words: Penta-substituted Cyclohexanol; Crystal Structure; Weak interactions; DFT Study

1. Introduction

Crystal engineering is the understanding of intermolecular interactions in the context of crystal packing and the utilization of such understanding in design of new solids with desired physical and chemical properties [1]. Over the past 50 years, Crystal engineering has grown and developed as a natural outcome of the interplay between crystallography and chemistry [2, 3]. Chemistry deals with molecules while crystallography with crystals, which are extended, ordered assemblies of molecules. The interplay between chemistry and crystallography is therefore the interplay between the structure and properties of molecules on one hand and those of extended assemblies of molecules on the other [4]. The main initiative of "crystal engineering" is the design of periodic structures with a desired supramolecular organization that makes it possible to achieve or modify a desired property in the created material. Crystal engineering includes three distinct activities, which form a continuous sequence: 1) the study of intermolecular interactions; 2) the study of packing modes, in the context of these interactions and with the aim of defining a design strategy; and 3) the study of crystal properties and their fine-tuning with deliberate variations in the packing. Besides hydrogen bonding, the C-–H$\cdots \pi$ [5, 6], $\pi \cdots \pi$ [7–9], interactions are also the important molecular forces whose nature is still a matter of discussion. These types of interactions undoubtedly play important roles in determining the crystal packing, molecular assemblies and structures of large biological systems [10, 11].

Moreover, aromatic rings can interact in different geometrical arrangements, for example, face-to-face, offset, and point-to-face [12], and have been found to be a useful tool in the manipulation of the molecular components in crystals. The $\pi \cdots \pi$, C–H$\cdots \pi$ interactions, as well as H-bonding interactions are also widely regarded as stabilizing interactions for a number of bio(macro)molecules, molecular recognition and supramolecular assemblies. At present, these types of noncovalent interactions play a pivotal role in modern chemical research and considered as backbones of supramolecular chemistry, material science and even biochemistry. One point should be mentioned here—experimental investigations showed that the strength of π-π interaction is maximum in presence of electron withdrawing substituents or heteroatoms. The electron withdrawing nature of these substituents decreases the π-electron density in the rings and consequently the π-electron repulsion. Although Li et. al. reported [13] only the

---

*corresponding author—Saugata Konar, mail id: saugata.konar@gmail.com, Sudipta Pathak, mail id: sudiptachemster@gmail.com

synthesis of this class of compounds but not the X-ray crystal structure and well-organized weak interactions of bromo derivative of penta substituted cyclohexane.

By considering of this, we have reported first X-ray crystal structure of bromo derivative of penta-substituted cyclohexanol **(A)** and the single-crystal X-ray structural analysis of **A** revealed remarkable supramolecular architecture guided by various weak forces like $\pi \cdots \pi$, C–H$\cdots \pi$, Br$\cdots$Br and hydrogen bonding. The crystal as a whole is an organization of different kind of supramolecular interactions. We have also provided the plausible mechanism for the formation of compound **A**. In addition, our present work combines DFT (Density Function Theory) optimized structure and experimentally obtained X-ray crystal structure. An in-depth structural analysis of the present compound is fully described here.

2. Experimental methods

2.1 General methods and materials

All reagents and chemicals were of AR grade and obtained from commercial sources (SD Fine Chemicals, India; and Aldrich) and used without further purification.

2.2 Synthesis of compound A [(1S,2S,3R,4S,6S)-2,6-bis(4-bromrophenyl)-4-hydroxy-4-(pyridin-2-yl)cyclohexane-1,3-diyl)-bis(pyridin-2-ylmethanone)]

The compound '**A**' was synthesized by reported method [13].

2.3 Synthesis of X-ray crystal structure of A

Firstly, white compound '**A**' of definite quantity (1 mmol, 0.695 g) was dissolved in 20 cm^3 DMF: H_2O (1 : 1) solvent and stirring was continued for two hours. After two hours the solution turned cleared. It was left for slow evaporation at room temperature. After 2 weeks colorless X-ray quality crystals of **A** separated out and they were collected by the usual technique. (Yield: 74%).

2.4 Crystallographic data collection and refinement

Selected crystal data for **A** is given in Table 1 and selected metrical parameter of the complex is given in Table 2. Data collections were made using Bruker SMART APEX II CCD area detector equipped with graphite monochromated Mo Kα radiation (λ = 0.71073 Å) source in φ and

ω scan mode at 293(2) K for both. Cell parameters refinement and data reduction were carried out using the Bruker SMART APEX II. Cell parameters refinement and data reduction were carried out using Bruker SMART [14] and Bruker SAINT softwares for all the complexes. The structure of all the complexes were solved by conventional direct methods and refined by full-matrix least square methods using F2 data. SHELXS-97 and SHELXL-97 programs [15] were used for structure of all the complexes solution and refinement respectively.

Table 1: Experimental Crystallographic Data for A

Formula	C$_{35}$H$_{27}$Br$_2$N$_3$O$_3$
Formula weight	697.40
Crystal system	Triclinic
Space group	P-1
a/Å	9.5725(3)
b/Å	10.7005(4)
c/Å	15.9974(5)
α/°	92.772(2)
β/°	97.442(2)
γ/°	103.645(2)
V/Å^3	1573.66(9)
Z	2
D_c/g cm^{-3}	1.472
μ/mm^{-1}	2.615
$F(000)$	400
θ range/°	1.97–25.02
Reflections collected	16876
Unique reflections	5511
Reflections $I > 2\sigma(I)$	3713
R_{int}	0.0457
Goodness-of-fit (F^2)	0.982
$R_1(I > 2\sigma(I))^a$	0.0779
wR_2^b	0.1426
Δ_ρ max / min /eÅ^3	−0.51, 0.62
$^a R_1 = \sum \|F_o\| - \|F_c\| / \sum \|F_o\|$, $^b wR_2 = [\sum(w(F_o^2 - F_c^2)^2) / \sum w(F_o^2)^2]^{1/2}$.	

2.5 Computational details

Ground state electronic structure calculations in gas phase of the ligand has been carried out using

DFT [16] method associated with the conductor-like polarizable continuum model (CPCM) [17]. Becke's hybrid function [18] with the Lee-Yang-Parr (LYP) correlation function [19] was used for the study. For C, H, N, O and Br atoms we employed $6-31+$ (g) as basis set for all the calculations. The calculated electron-density plots for frontier molecular orbitals were prepared by using Gauss View 5.1 software. All the calculations were performed with the Gaussian 09W software package [20].

3. Results and discussion

3.1 Crystal structure description of Compound A

Single–crystal X-ray diffraction analysis reveals that compound **A** is neutral, mononuclear compound and crystallizes in a triclinic system in the space group P-1 with $Z = 2$. The unit cell of **A** is comprised of two molecules. The molecular structure of **A** is depicted in Fig. 1 with the atom numbering schemes; selected bond lengths and angles of **A** are given in the caption of Table 2. There is a six membered chair shaped cyclohexane system at the centre of this molecule. There are two *p*-bromo phenyl groups, attached at the equatorial position of the C8 and C10 carbons of the cyclohexane ring. The axial and equatorial positions of C9 and C7 carbons of cyclohexane ring are occupied by pyridine-2-carboxy group. The axial position of C12 carbon of cyclohexane is occupied by hydroxyl group whereas the equatorial position of the same carbon is occupied by 2-pyridine group.

Table 2: Selected bond distances (Å) and angles (°) data for A

Selected Bonds	Bond Lengths (Å)	Selected Bond Angles	(°)
Br1–C21	1.905(3)	C21–C22–C23	118.4(4)
Br2–C33	1.894(4)	C22 C23 C18	121.5(4)
C22–C21	1.364(5)	C13 N1 C17	117.9(4)
C22–C23	1.383(5)	C20 C21 C22	122.2(3)
C23–C18	1.387(5)	C20 C21 Br1	117.8(3)
O2–C6	1.210(4)	C22 C21 Br1	120.0(3)
N1–C13	1.306(5)	C19 C18 C23	117.8(3)
N1–C17	1.354(6)	C19 C18 C10	119.2(3)
O3–C12	1.426(5)	C23 C18 C10	122.9(3)
C21–C20	1.363(5)	C18 C10 C11	114.4(3)
C18–C19	1.364(5)	C18 C10 C9	111.0(3)
C18–C10	1.522(5)	C11 C10 C9	110.9(3)
C10–C11	1.527(5)	C24 C9 C8	113.0(3)
C10–C9	1.555(5)	C24 C9 C10	110.7(3)
C9–C24	1.516(5)	C8 C9 C10	109.5(3)
C9–C8	1.545(4)	C29 N3 C25	116.1(4)
N3–C29	1.323(5)	N3 C29 C28	123.9(5)
N3–C25	1.327(5)	C21 C20 C19	118.1(4)
C29–C28	1.367(7)	C18 C19 C20	121.9(4)
C20–C19	1.393(5)	C30 C8 C7	113.8(3)
C8–C30	1.512(5)	C30 C8 C9	110.6(3)
C8–C7	1.531(5)	C7 C8 C9	112.4(3)
C7–C6	1.525(4)	C6 C7 C8	110.6(3)
C7–C12	1.545(5)	C6 C7 C12	109.7(3)
C6-C5	1.509(5)	C8 C7 C12	111.7(3)

Selected Bonds	Bond Lengths (Å)	Selected Bond Angles	(°)
C5–C4	1.325(5)	O2 C6 C5	119.7(3)
C5–N2	1.389(6)	O2 C6 C7	122.1(3)
N2–C1	1.428(7)	C5 C6 C7	118.2(3)
C1–C2	1.361(8)	C4 C5 N2	124.4(4)
C2–C3	1.359(7)	C4 C5 C6	117.5(3)
C11–C12	1.524(5)	N2 C5 C6	118.1(4)
C12–C13	1.534(5)	C5 N2 C1	114.8(5)
C25–C26	1.363(5)	C2 C1 N2	120.4(5)
C25-C24	1.504(5)	C3 C2 C1	117.8(5)
C26–C27	1.376(7)	C12 C11 C10	111.7(3)
C30–C31	1.385(5)	O3 C12 C11	106.5(3)
C30–C35	1.392(5)	O3 C12 C13	109.5(3)
C31–C32	1.392(5)	C11 C12 C13	110.2(3)
C32–C33	1.362(5)	O3 C12 C7	109.9(3)
C33–C34	1.381(6)	C11 C12 C7	110.7(3)
C34–C35	1.377(6)	C13 C12 C7	110.0(3)
C4–C3	1.307(6)	N3 C25 C26	123.5(4)
C13–C14	1.381(5)	N3 C25 C24	118.4(3)
C17–C16	1.332(6)	C26 C25 C24	118.1(4)
C16–C15	1.343(7)	C25 C26 C27	119.3(5)
C15–C14	1.391(6)	C31 C30 C35	117.2(4)
C27–C28	1.352(8)	C31 C30 C8	123.2(3)
C24–O1	1.216(4)	C35 C30 C8	119.6(3)
		C30 C31 C32	121.7(4)
		C33 C32 C31	119.1(4)
		C32 C33 C34	121.0(4)
		C32 C33 Br2	119.8(3)
		C34 C33 Br2	119.2(3)
		C35 C34 C33	119.2(4)
		C34 C35 C30	121.7(4)
		C3 C4 C5	117.7(4)
		C4 C3 C2	124.9(5)
		N1 C13 C14	121.6(4)
		N1 C13 C12	116.2(3)
		C14 C13 C12	122.2(3)
		C16 C17 N1	123.8(4)
		C17 C16 C15	119.1(4)
		C16 C15 C14	118.8(5)
		C13 C14 C15	118.9(4)

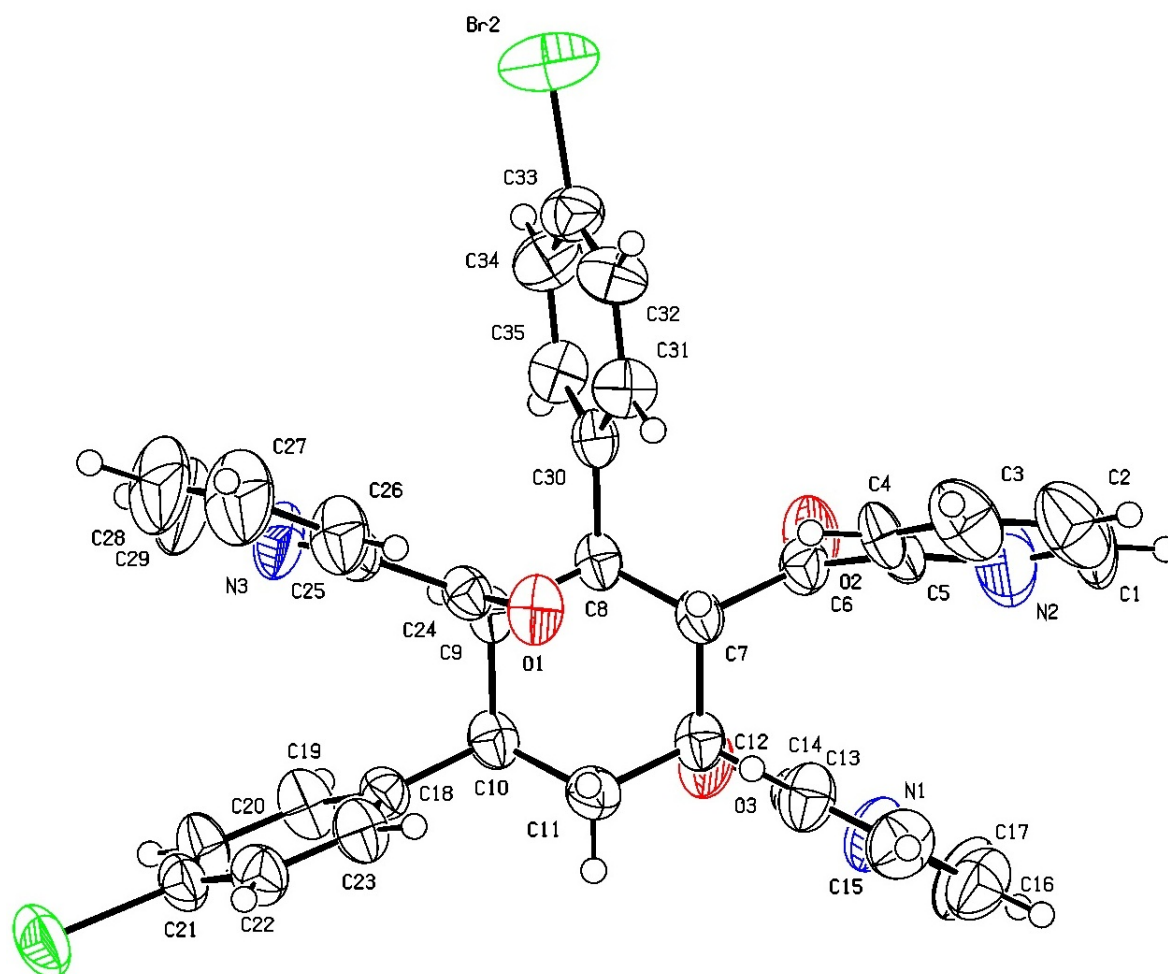| Selected Bonds	Bond Lengths (Å)	Selected Bond Angles	(°)
		C28 C27 C26	117.7(5)
		C27 C28 C29	119.4(5)
		O1 C24 C25	117.9(3)
		O1 C24 C9	121.4(3)
		C25 C24 C9	120.6(3)

Fig. 1. The single crystal X-ray structure of **A** (The thermal ellipsoid plot has been drawn with 50% ellipsoidal probability).

3.2 Mechanistic pathway

Compound **A** is formed by equivalent amount of 2-Acetylpyridine and 4-bromobenzaldehyde under the condition of NaOH solution in ethanol/H_2O mixture (Scheme 1). The plausible mechanism for the formation of compound **A** is as follows (Scheme 2): when 2-Acetylpyridine (1) is treated with NaOH, enolate 2 is formed. Enolate **2** takes part in aldol condensation reaction with aromatic aldehyde **3** to get β-hydroxycarbonyl compound **4**. The compounds **4** generates very stable α,β-unsaturated carbonyl compound **5** after dehydration. Compound **5** participates in Michael addition with enolate **2** to get compound **6** which abstracts proton from water to obtain compound **7**. Enolate **6** which is further obtained when compound **7** reacts with NaOH; participates in aldol condensation reaction with aromatic aldehyde 3 to obtain compound **8**. Compound **8** abstracts proton from water to acquire compound **8** which takes proton form water to obtain β-hydroxy carbonyl

compound **9**. Dehydration of compound **9** generates compound **10** which participates in Michael addition with enolate **2** to furnish compound **11**. Then compound **11** converts to compound **12** after proton abstraction from water. Finally eno-
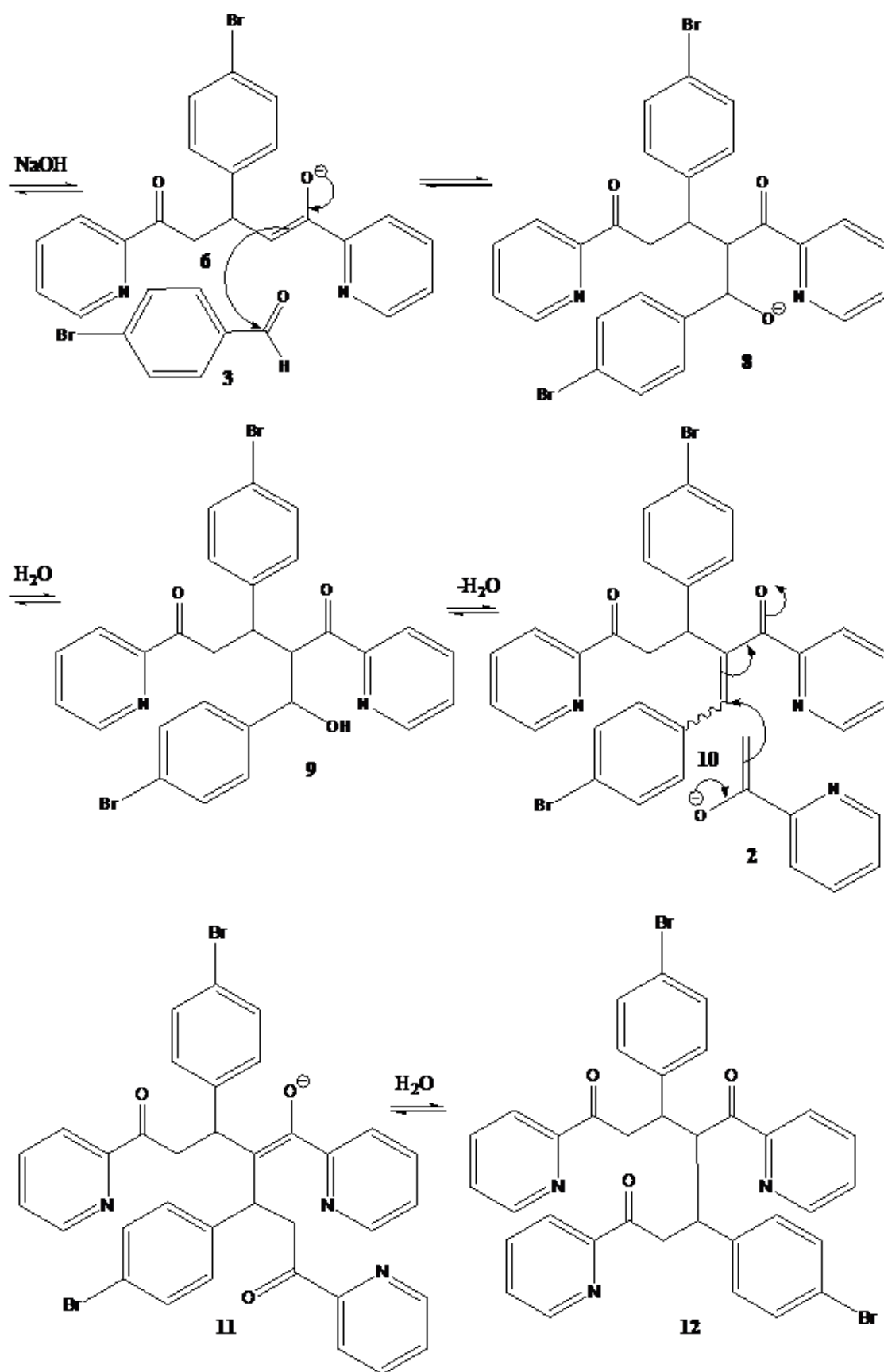
late **13** (enolate of compound **12**) takes part in intramolecular aldol condensation to get compound **A**. Though there is a possibility to get dehydration of compound A, still this is not occurring due to sterically crowded cyclohexene formation.
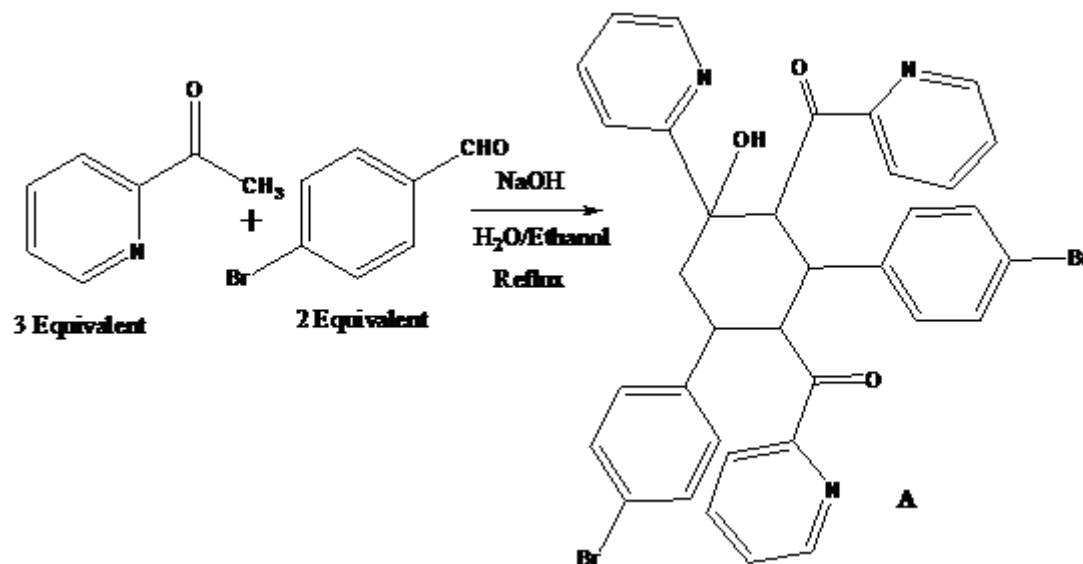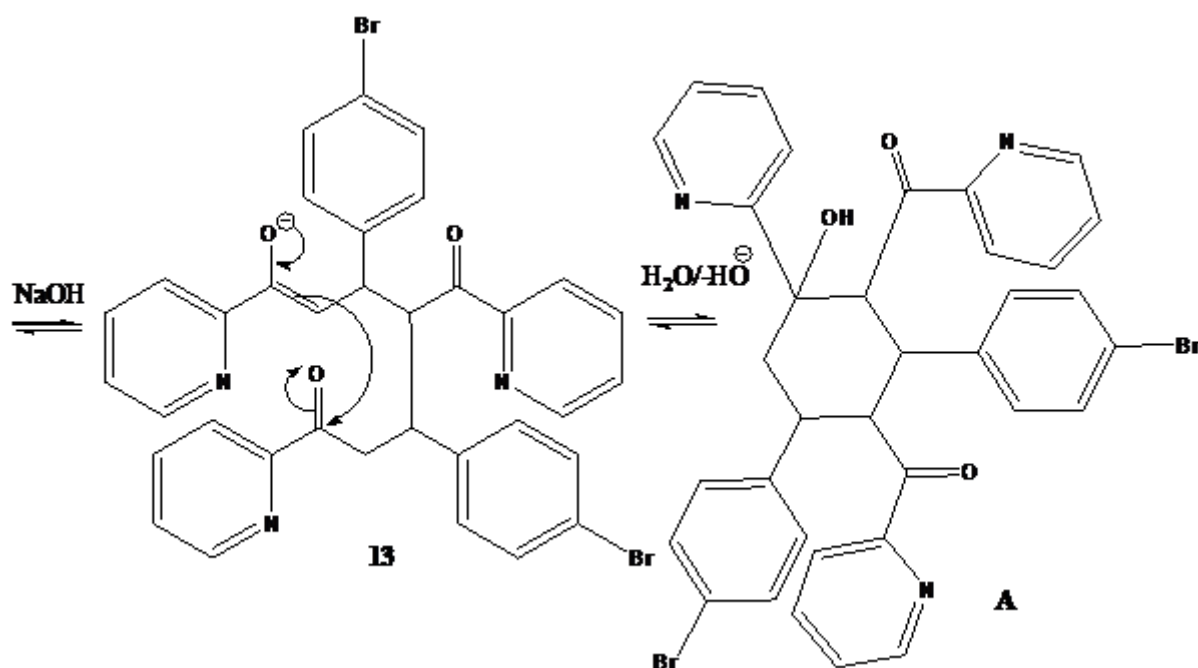

Scheme 1. Synthesis of compound A via tandem aldol reaction.
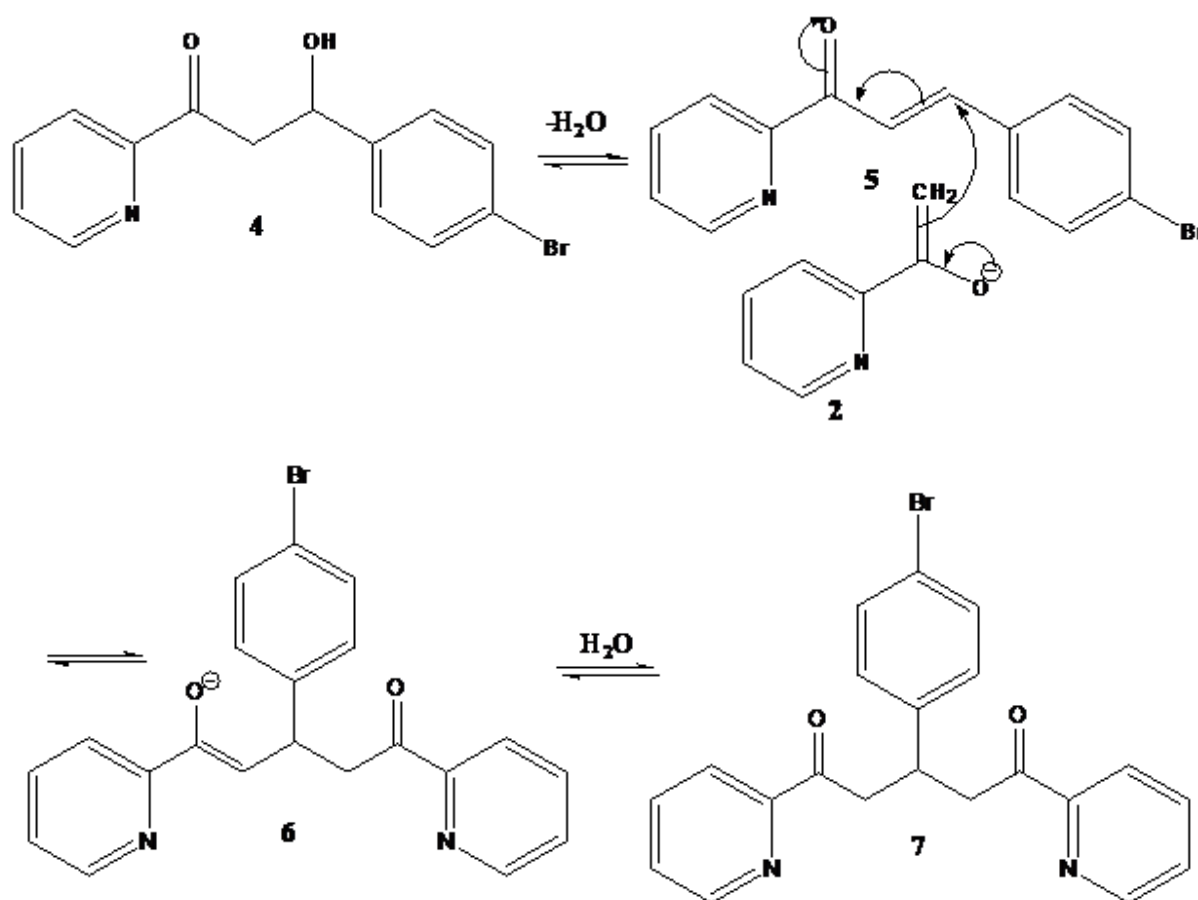
Scheme 2. Plausible mechanism for the formation of compound **A**.

3.3 Weak interactions

The compound **A** shows different kinds of weak interactions like $\pi \cdots \pi$ interaction, C-H$\cdots \pi$ interaction, Br$\cdots$Br interaction and H-bonding interaction in solid state structure that contributes to the self assembly process. The formation of a supramolecular $\pi \cdots \pi$ interaction is ensured
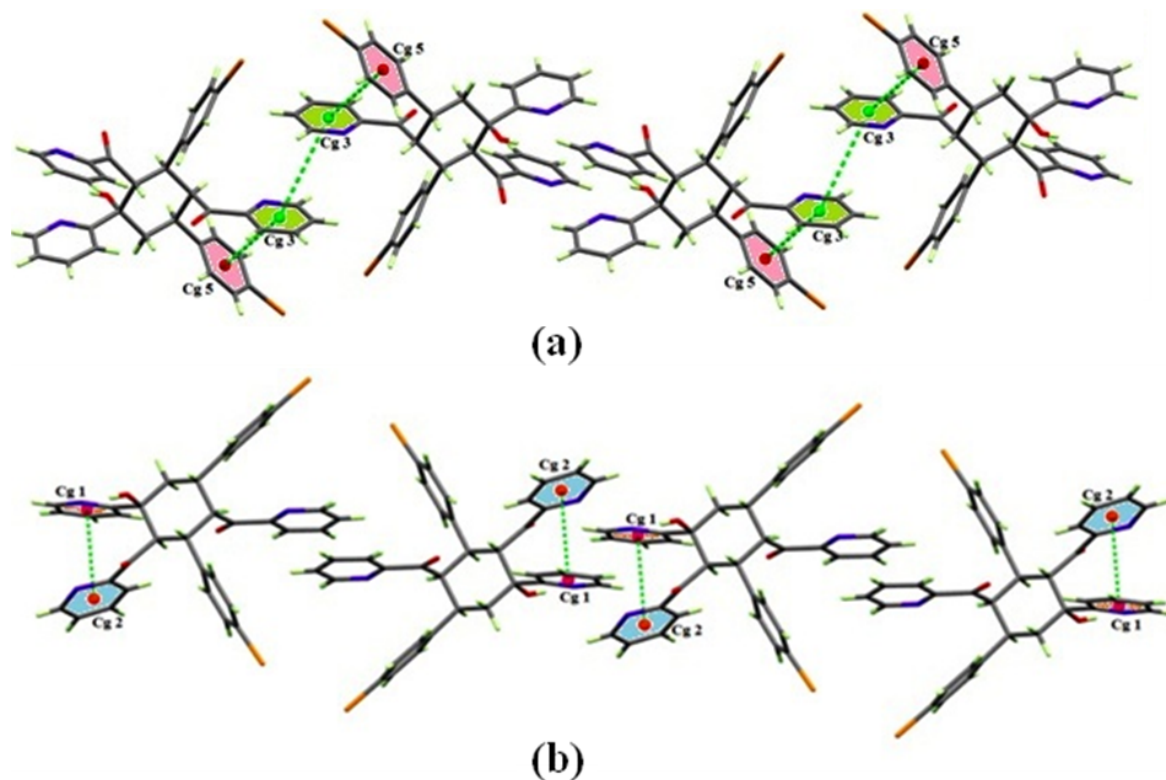

Fig. 2. Three different types of $\pi \cdot \pi$ interactions exhibited by Compound **A**.

mainly by three types (Fig. 2). Firstly, the aromatic ring, Cg3, N3-C25-C26-C27-C28-C29, is stacked over same aromatic ring Cg3 of neighboring molecule of symmetry 1-X, 1-Y, 1-Z (4.533 Å). Secondly, the Cg3 aromatic ring is stacked over of different aromatic ring Cg5, C18-C19-C20-C21-C22-C23 of neighboring molecule of symmetry X, Y, Z (4.367 Å) (Fig. 2a). Thirdly, the aromatic

ring, Cg1, N1-C13-C14-C15-C16-C17, is stacked over different moiety Cg2, N2-C1-C2-C3-C4-C5 of same molecule (3.841 Å) (Fig. 2b). Fig. 3 is depicting the weak Br···Br interaction and C-H···π interactions within the packing diagram. Here, H-bonding is observed mainly of intermolecular types. All C–H···π, Br···Br and H-bonding interactions can form a supramolecular 1D chain.
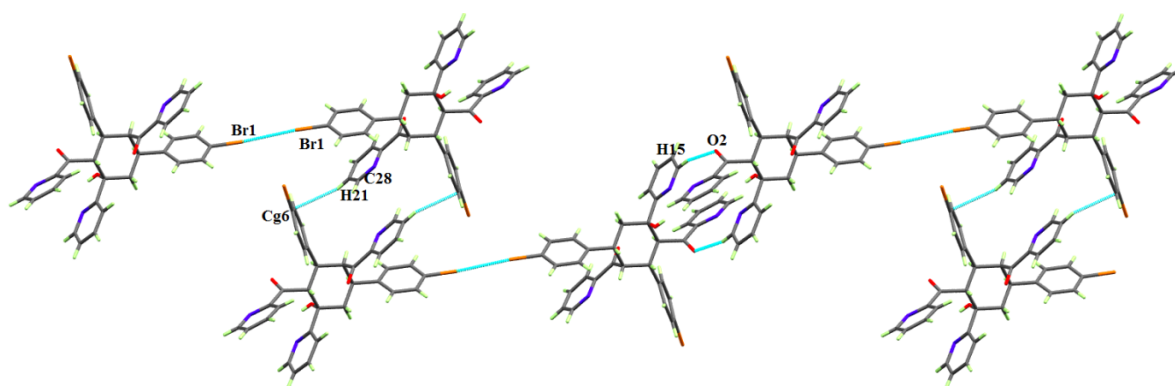

Fig. 3. 1D chain formed by Br···Br interaction, C-H···π interaction and H-bonding interaction in compound **A**.

Table 3: Geometric Features (distances in Å and angles in degrees) of the π···π Interactions Obtained for Compound A.

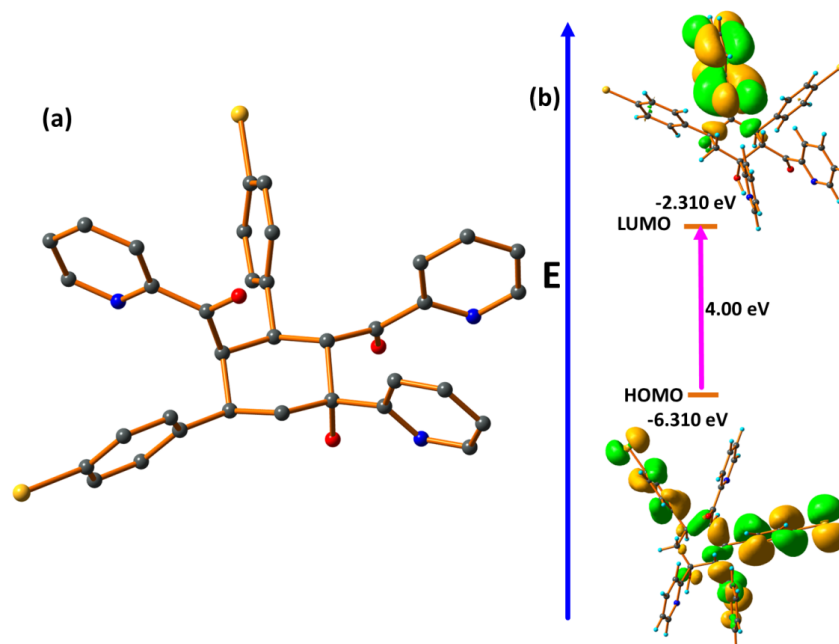| Compound	Cg(Ring I)…Cg(Ring J)	Cg…Cg	Cg(I)…Perp	Cg(J)…Perp	α	β	γ	Symmetry
	Cg1…Cg2	3.841(3)	3.797	3.523	29.53	23.46	8.67	X, Y, Z
S	Cg3…Cg3	4.533(3)	3.277	3.277	0.00	43.71	43.71	1-X, 1-Y, 1-Z
	Cg3…Cg5	4.367(3)	4.101	3.357	42.92	39.76	20.08	X, Y, Z

Fig. 4. (a) Geometry optimized molecular structure of molecule A and (b) its HOMO-LUMO energy differences.

3.4 Geometry optimization and electronic structure

The optimized geometries for molecule **A** is shown in Fig. 4a. The composition of the **A** is confirmed from Single crystal X-ray structure and then per-formed the theoretical geometry optimization on it. The positive and negative phases are represented in orange and green colour, re-spectively. The HOMO-LUMO energy gap is ΔE = 4.00 eV (Fig. 4b). The molecular orbitals are shown in Fig. 5.
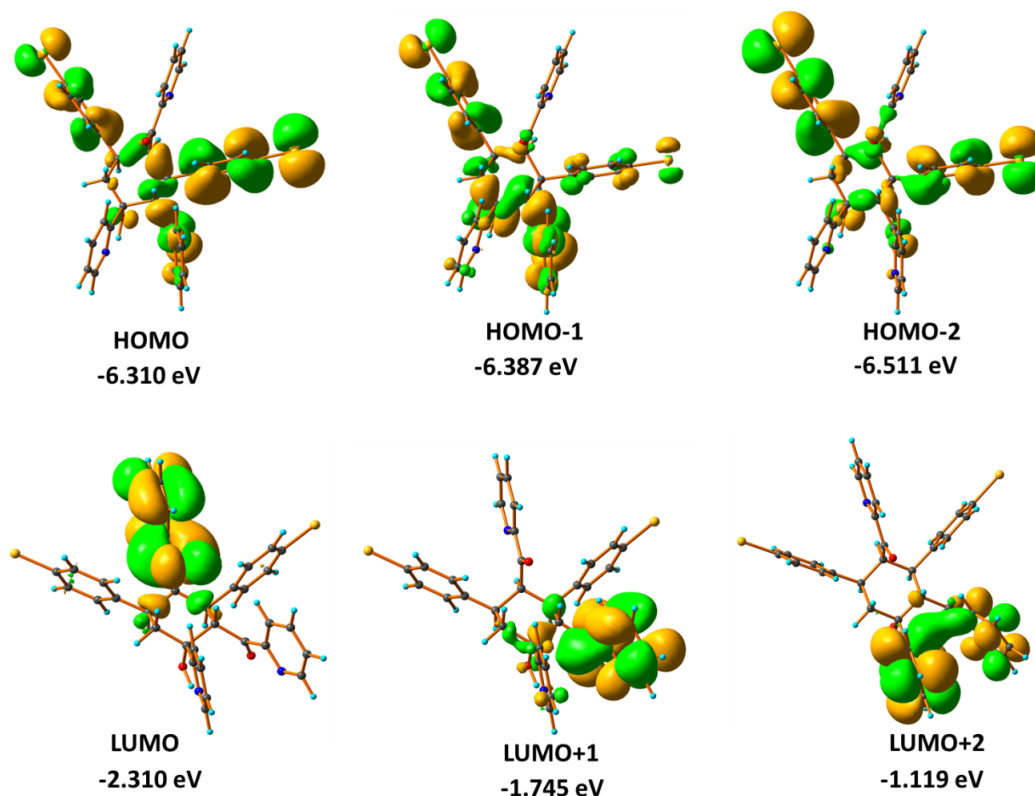

HOMO
-6.310 eV

HOMO-1
-6.387 eV

HOMO-2
-6.511 eV

LUMO
-2.310 eV

LUMO+1
-1.745 eV

LUMO+2
-1.119 eV

Fig. 5. The frontier molecular orbitals of molecule A.

4. Conclusion

During work using the compound (1S,2S,3R,4S,6S)-2,6-bis(4-bromrophenyl)-4-hydroxy-4-(pyridin-2-yl)cyclohexane-1,3-diyl)-bis(pyridin-2-ylmethanone) **(A)**, we have serendipitously crystallized this said compound. The DFT study has been used to compare ex-perimentally found X-ray crystal structure with optimized geometry. In the framework of organic compound, various supramolecular interactions, like $\pi \cdots \pi$, C–H$\cdots \pi$, Br$\cdots$Br and H-bonding interactions are present and these imperative interactions play crucial roles in the construction of extended networks in this framework. One of the most important aspects of the theoretical analysis is the elucidation of the contributions to molecular recognition and self-assembly by assigning discrete energy values to them. This will provide helpful information to researchers working on supramolecular chemistry, crystal engineering or drug design to develop energy scoring functions.

Appendix A. Supplementary data

CCDC 2111567 contains the supplemen-tary crystallographic data for **A**. These data can be obtained free of charge via http://www.ccdc.cam.ac.uk/conts/retrieving.html, or from the Cambridge Crystallographic Data Centre, 12 Union Road, Cambridge CB2 1EZ, UK; fax: (+44) 1223-336-033; or e-mail: de-posit@ccdc.cam.ac.uk.

Conflict of interest

The authors declare no conflict of interest.

References

[1] G R Desiraju, Crystal Engineering: From Molecule to Crystal, J. Am. Chem. Soc., 135, 9952–9967 (2013).

[2] A D Bond, Pharmaceutical crystallography: is there a devil in the details? CrystEngComm, 14, 2363–2366 (2012).

[3] A I Cooper, Molecular organic crystals: from barely porous to really porous, Angew. Chem. Int. Ed., 51, 7892–7894 (2012).

[4] J D Dunitz, X-Ray Analysis and the Structure of Organic Molecules; Cornell University Press: Ithaca, NY (1979).

[5] M Kumar and P V Balaji, C-H...pi interactions in proteins: Prevalence, pattern of occurrence, residue propensities, location, and contribution to protein stability, J. Mol. Model, 20: 2136 (1–14) (2014).

[6] Y Ruan, P W Peterson, C M Hadad and J D Badjić, On the encapsulation of hydrocarbon components of natural gas within molecular baskets in water. The role of C–H$\cdots\pi$ interactions and the host's conformational dynamics in the process of encapsulation, Chem. Commun., 50, 9086–9089 (2014).

[7] C D M Churchill, L R Rutledge and S D Wetmore, Effects of the biological backbone on stacking interactions at DNA–protein interfaces: the interplay between the backbone$\cdots\pi$ and $\pi\cdots\pi$ components, Phys. Chem. Chem. Phys., 12, 14515–14526 (2010).

[8] R F Semeniuc, T J Reamer and M D Smith, 8-Quinoline based ligands and their metallic derivatives: A structural and statistical investigation of quinoline – stacking interactions, New J. Chem. 34, 439–452 (2010).

[9] W Wang, Y Zhang and Y –B Wang, Noncovalent $\pi\cdots\pi$ interaction between graphene and aromatic molecule: Structure, energy and nature, J. Chem. Phys., 140, 94302 (2014).

[10] S Banerjee, N N Adarsh and P Dastidar, An unprecedented all helical 3D network and a rarely observed non-interpenetrated octahedral network in homochiral Cu(II) MOFs: effect of steric bulk and $\pi-\pi$ stacking interactions of the ligand backbone, CrystEngComm, 11, 746–749 (2009).

[11] H R Khavasi and M Azizpoor Fard, $\pi-\pi$ interactions affect coordination geometries, Cryst. Growth Des., 10, 1892–1896 (2010).

[12] J -Y Wu, H -Y Hsu, C -C Chan, Y -S Wen, C Tsai and K –L. Lu, Formation of Infinite Linear Mercury Metal Chains Assisted by Face-to-Face $\pi-\pi$ (Aryl−Aryl) Stacking Interactions, Cryst. Growth Des., 9, 258–262 (2009).

[13] C -W Li, T -H Shen and T -L Shih, Reinvestigation of synthesis of halo-substituted 3-phenyl-1-(2-pyridyl)-2-propen-1-ones (azachalcones). A tandem reaction for formation of penta-substituted cyclohexanols Tetrahedron (2017), DOI: 0.1016/j.tet.2017.06.033.

[14] Bruker, SMART v5. 631, Bruker AXS Inc., Madison, W I, USA, 2001.

[15] G M Sheldrick, SHELXS-97 and SHELXL-97, University of Göttingen, Göttingen, Germany, 1997.

[16] R G Parr and W Yang, Density Functional Theory of Atoms and Molecules, Oxford University Press, Oxford (1989).

[17] V Barone and M Cossi, Quantum Calculation of Molecular Energies and Energy Gradients in Solution by a Conductor Solvent Model, J. Phys. Chem. A, 102, 1995–2001 (1998).

[18] A D Becke, Density-functional thermochemistry. III. The role of exact exchange, J. Chem. Phys., 98, 5648 (1993).

[19] C Lee, W Yang and R G Parr, Development of the Colle-Salvetti correlation-energy formula into a functional of the electron density, Phys. Rev. B, 37, 785 (1998).

[20] M J Frisch, G W Trucks, H B Schlegel, G E Scuseria, M A Robb, J R Cheeseman, G Scalmani, V Barone, B Mennucci, G A Petersson, H Nakatsuji, M Caricato, X Li, H P Hratchian, A F Izmaylov, J Bloino, G Zheng, J L Sonnenberg, M Hada, M Ehara, K Toyota, R Fukuda, J Hasegawa, M Ishida, T Nakajima, Y Honda, O Kitao, H Nakai, T Vreven, J A Montgomery Jr., J E Peralta, F Ogliaro, M Bearpark, J J Heyd, E Brothers, K N Kudin, V N Staroverov, R Kobayashi, J Normand, K Raghavachari, A Rendell, J C Burant, S S Iyengar, J Tomasi, M Cossi, N Rega, J M Millam, M Klene, J E Knox, J B Cross, V Bakken, C Adamo, J Jaramillo, R Gomperts, R E Stratmann, O Yazyev, A J Austin, R Cammi, C Pomelli, J W Ochterski, R L Martin, K Morokuma, V G Zakrzewski, G A Voth, P Salvador, J J Dannenberg, S Dapprich, A D Daniels, Ö Farkas, J B Foresman, J V Ortiz, J Cioslowski and D J Fox, Gaussian Inc., Wallingford CT (2009).